Available online at www.sciencedirect.com
SCIENCE DIRECT
Thermochimica Acta 447 (2006) 81–88
thermochimica acta
www.elsevier.com/locate/tca

DSC and Raman studies of the side chain length effect of ubiquinones on the thermotropic phase behavior of liposomes

Yann Roche [1], Pierre Peretti, Sophie Bernard *

Paris Descartes University, Biomedical Research Center, Laboratoire de Neuro-Physique Cellulaire, EA 3817, 45 rue des Saints-Pères, 75270 Paris Cedex 06, France

Received 21 March 2006; received in revised form 5 May 2006; accepted 15 May 2006
Available online 20 May 2006

Abstract

Differential scanning calorimetry and Raman spectroscopy have been used to examine the effects of ubiquinones (UQ*n*) on the thermotropic phase behavior of dipalmitoylphosphatidylcholine (DPPC) in multilamellar vesicles, for UQ/DPPC molar ratios ranging from 0.01 to 0.1. The influence of the side chain length has been investigated by comparing the effect of a series of UQ with 2 (UQ2), 4 (UQ4), 6 (UQ6) and 10 isoprene units (UQ10).

In the presence of increasing amount of UQ2 or UQ4, concomitant shift of the gel to liquid crystalline phase transition towards lower temperatures and vanishing of the pretransition are observed. Short-chain ubiquinones are thus inserted parallel to phospholipid chains, their benzoquinone ring being close to the DPPC polar headgroups. In addition, broadening and skewing of the main transition peak support the fact that UQ2 and UQ4 are laterally self-organized in highly concentrated regions located at the boundary of lipid domains. The lipid thermotropic behavior is not affected by the presence of other analogues of the series, UQ6 and UQ10. They remain homogeneously dispersed within the midplane of the phospholipid bilayer. Such a chain length dependence on the location and the organization of ubiquinones analogues may be correlated with their biological activities in biomembranes.

Keywords: Ubiquinones; Phospholipid bilayer; Liposomes; Differential scanning calorimetry; Raman scattering

1. Introduction

Ubiquinones (UQ*n* or coenzymes Q) [1–5] act as lipophilic electron carriers diffusing between enzymatic complexes in the respiratory chains of mitochondrial [6] and bacterial [7] membranes. They consist of a redox active 2,3-dimethoxy-5-methylbenzoquinone ring with a hydrophobic isoprenoid chain in position 6 (see Fig. 1). Ubiquinones differ from one to the other in the chain length of their side chain as indicated by a number (*n*) following the name which ranges between 2 and 10 isoprene units (2-methyl-2-butene) [8,9]. These key components mediate the electron transfer in the mitochondrial inner membrane and also participate in the translocation of protons across the membrane [10,11]. Apart from this bioenergetic function, ubiquinols, the reduced form of UQ*n*, are important natural antioxidants, preventing biomolecules from peroxidation [3]. Indeed, ubiquinols can inhibit peroxidation by reaction with $ROO^{\bullet}$ radicals [12,13], or regenerate Vitamin E, another important liposoluble antioxidant [14]. More recently, roles in the control of cell growth [15–17] and apoptosis [18,19] have also been reported.

Studying the location and the molecular organization of ubiquinones with different chain length in model membranes can lead to the interpretation of their biological functions. In a previous paper [20], we studied mixed monomolecular films containing phospholipids and UQ2 or UQ10. Our conclusions pointed out that UQ2 tended to have their benzoquinone rings located nearer the headgroup of phospholipids, their side chain parallel to phospholipid acyl chains, while UQ10 seemed to lie parallel to the membrane plane in the bilayer center. Similar conclusions were drawn by authors using phospholipid bilayers as model membranes and techniques such as ^{1}H NMR [21], NMR

* Corresponding author. Tel.: +33 1 42862046; fax: +33 1 42862085.
E-mail address: Sophie.Bernard@univ-paris5.fr (S. Bernard).
[1] Present address: URCA-UMR CNRS 6142, Unité MéDIAN, UFR de Pharmacie, 51 rue Cognacq-Jay, 51096 Reims Cedex, France.

0040-6031/$ – see front matter © 2006 Elsevier B.V. All rights reserved.
doi:10.1016/j.tca.2006.05.009

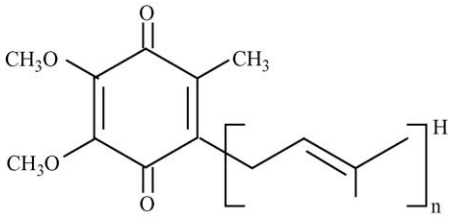

Fig. 1. Molecular structure of ubiquinones: $n = 2$, UQ2; $n = 4$, UQ4; $n = 6$, UQ6; $n = 10$, UQ10.

measurements of ^{13}C-labeled ubiquinones [22], linear dichroism and fluorescence quenching experiments [23,24], and combination of differential scanning calorimetry and X-ray diffraction analysis [25]. More recently, comparison of prenylquinones effectiveness in perturbation of the lipid thermotropic properties was studied by differential scanning calorimetry and gave results consistent with this model of short- and long-chain dependence on ubiquinone location in membrane [26]. Finally, Hauss et al. [27] have shown by neutron diffraction experiments that the polyisoprene domain of UQ10 and of squalane [28], lie in the center of the hydrophobic core parallel to the membrane plane and not parallel to the lipid chains. Thus, in addition to their biological roles, quinone polyisoprenoids may inhibit proton leakage.

However, these studies have mostly focused on the influence of short and long isoprenoid chains only, with little consideration regarding the interaction of middle chain homologues ($3 < n < 7$). Additionally, the possibility of a lateral organization of ubiquinones within membranes was recently raised [29] and remains to be extensively studied in model membranes. This concept takes into account the notion that UQ10 may not entirely exist in the freely diffusible, unbound form in the mitochondrial membranes and may instead be distributed in separate and distinct pools [30,31]. Thus, the present study aims to compare the interaction of a series of ubiquinones with 2 (UQ2), 4 (UQ4), 6 (UQ6) and 10 isoprene units (UQ10), with dipalmitoylphosphatidylcholine (DPPC) in multilamellar vesicles, using combination of differential scanning calorimetry (DSC) and Raman spectroscopy.

The thermotropic behavior of phospholipids is highly sensitive to the presence of foreign substances able to alter the lipid packing within the bilayer [32]. Differential scanning calorimetry (DSC) is the prevailing calorimetric method to investigate the thermotropic phase behavior of liposomes and monitor the effect of host molecules on the gel to liquid crystalline acyl chains melting transition [32–36]. Spectroscopic techniques, such as Raman spectroscopy, can provide information about chains melting but also about interchain interactions by plotting the ratio intensities of some characteristic Raman bands versus temperature [37–41]. DSC and Raman spectroscopy constitute powerful, non-invasive and complementary techniques to explore the organization of biological substances in lipid bilayers. Hence, by combining DSC and Raman data, we can investigate the type of interaction, the depth of the penetration into the bilayer, as well as the hydrocarbon chain structures.

2. Materials and methods

2.1. Materials

DPPC (synthetic, L-α type, purity grade 99%) was purchased from Sigma (France). UQ2 (synthetic, purity grade 98%), UQ6 (natural) and UQ10 (synthetic, purity grade 98%) were also obtained from Sigma, while UQ4 (synthetic, purity grade 95%) was from Fluka (France).

Organic solvents (chloroform and methanol) were of HPLC grade and were purchased from Fisher Scientific (France). Ultrapure water was treated on an Elgastat UHQ 2 system (resistivity of 18 MΩ cm).

2.2. Liposome preparation

The pure DPPC and mixed UQ/DPPC multilamellar vesicles with molar ratio ranging from 0.01 to 0.1 were prepared as described in the following procedure. According to the nature of the experiment (DSC or Raman spectroscopy), the appropriate amounts of DPPC were weighed in small glass test tubes and then diluted in chloroform. When necessary, the adequate volume of UQ stock solutions was added to obtain mixtures containing the required UQ/DPPC molar ratios.

Then, the sample tubes were placed under a nitrogen gas flow and simultaneously heated at 55–60 °C. Once the solvent was completely evaporated, the tubes were stored in a desiccator under vacuum at room temperature for at least 2 h in order to eliminate any traces of solvent. Thus, a film of perfectly dehydrated lipids was formed on the wall of the glass tubes. The formation of multilamellar vesicles was then achieved by adding the appropriate volume of ultra-pure water or D_2O (Sigma) for Raman experiments. The samples were heated at 60 °C (i.e., above the temperature of the gel to liquid crystalline phase transition of pure DPPC) and vortexed (Vortex Top-mix, Bioblock, France) several times for about 15 min to obtain homogeneous multilamellar suspensions.

2.3. Differential scanning calorimetry

DSC measurements were performed using a Setaram DSC 111 model microcalorimeter (France). A heating rate of 0.5 °C min^{-1} in the 25–50 °C temperature range was chosen. The phospholipid vesicles were prepared as stated above, so that the final DPPC concentration was 75 mM. A volume of 18 μL of multilamellar suspensions was introduced into a specific pan (Setaram). Another pan containing 18 μL of water was used as reference. The accuracy for enthalpy changes is within 5% after DSC calibration.

2.4. Raman spectroscopy

Experiments were performed on a computerized Jobin Yvon Ramanor HG2S double monochromator spectrometer with a 2017 Spectra Physics Ar^+ laser. We used the 514.5 nm laser line with a power of 400 mW at the laser head, and the spectral resolution was approximately 4 cm^{-1}. The scattered light, detected

at a right angle from the incident light, was collected on the photocathode of a cooled photomultiplier (EMI) and amplified by a dc operational amplifier.

The phospholipid vesicles were prepared as stated above, so that the water concentration was always 83% D_2O weight with respect to the total weight of DPPC and UQ (i.e., in a full state of hydration). Samples were enclosed into sealed 1 mm diameter glass capillaries and placed into a small cryostat with nitrogen circulation and temperature regulation from the Société de Matériel Cryogénique (SMC-TBT, Air Liquide, France),

Samples were heated at 60 °C before cooling, equilibrated for 15 min at a lower temperature, and then heated for measurements. They were left to equilibrate for 10 min to stabilize the temperature before spectrum was recorded. Each spectrum was the average of five spectra, carried out with a step of 0.3 cm^{-1} and an integration time of 0.5 s.

3. Results

3.1. Pure DPPC liposomes

The DSC thermogram obtained by heating multilamellar vesicles of pure DPPC from 25 to 50 °C shows the two well-known endothermic transitions (Fig. 2): a pretransition at about 35 °C and a main transition at 41.1 °C. The pretransition arises from the conversion of a lamellar gel phase (L'_β) to a rippled gel phase (P'_β), whereas the higher temperature transition corresponds to a conversion of a P'_β phase to a lamellar liquid crystalline (L_α) phase [34].

We determined the thermodynamic parameters related to the main transition (i.e., the temperature at which the heat flow reaches its maximum): $T_m = 41.1 \pm 0.1$ °C, the cooperativity of the transition given by the peak width at half-height: $\Delta T_{1/2} = 0.30 \pm 0.05$ °C and the enthalpy of the transition determined from the area under DSC curve: $\Delta H = 30 \pm 1$ kJ mol^{-1}.

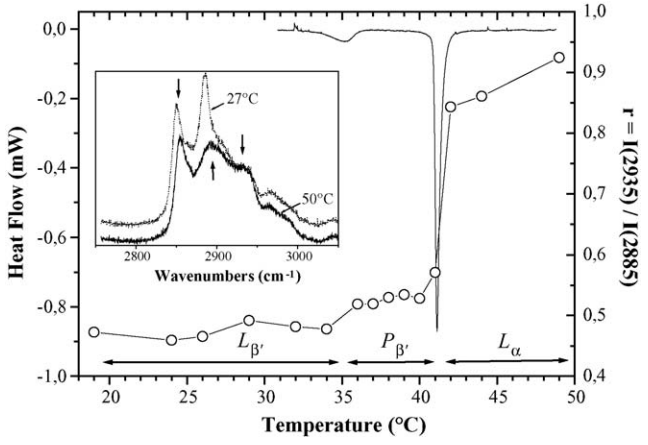

Fig. 2. DSC heating thermogram (solid line) and Raman intensity ratio r (symbols) of DPPC multilamellar vesicles in water. Both methods highlight the pretransition $L'_\beta \rightarrow P'_\beta$ and the main transition $P'_\beta \rightarrow L_\alpha$. (Inset) example of Raman spectra recorded at 27 °C (L'_β) and 50 °C (L_α). From left to right, vertical arrows indicate the position of $\nu_s(CH_2)$, $\nu_{as}(CH_2)$ and $\nu_s(CH_3)$ bands, respectively.

These values are in keeping with data reported in the literature [32,42]. Accuracy on T_m, ΔH and $\Delta T_{1/2}$ was evaluated from nine independent measurements carried out under the same conditions.

Raman spectra of multilamellar vesicles of pure DPPC were recorded in the C–H stretching mode region of the methyl and methylene groups of the alcyl chains of DPPC (2750–3050 cm^{-1}), for temperatures ranging from 20 to 50 °C. Bands located at 2850 and 2880 cm^{-1} correspond to the symmetric $\nu_s(CH_2)$ and antisymmetric $\nu_{as}(CH_2)$ C–H stretching vibration of the methylene groups of the acyl chains of DPPC, respectively. The band at 2935 cm^{-1} is a superposition of two vibrations. The former (2925 cm^{-1}) is the symmetric C–H stretching vibration of the methyl endgroups of the chains $\nu_s(CH_3)$ and the latter (2935 cm^{-1}) is an IR active band (Raman inactive). This band becomes Raman active upon heating because of symmetry changes as lipid chains change from all-*trans* conformation to *gauche* conformation [43]. The inset in Fig. 2 depicts the spectra obtained at 27 and 50 °C (i.e., before and after the main transition temperature, respectively). The appearance of *gauche* conformers leads to significant changes in the Raman spectrum of DPPC vesicles. The intensity of the $\nu_{as}(CH_2)$ mode, located at ca. 2880 cm^{-1}, significantly decreases as well as its spectral width and its frequency is slightly modified. Simultaneously, the intensity of the $\nu_s(CH_3)$ band at 2935 cm^{-1} increases. Lastly, the intensity of the $\nu_s(CH_2)$ mode located at ca. 2850 cm^{-1} does not vary, but its frequency increases slightly.

Fig. 2 shows the Raman intensity ratio $r = I_{2935}/I_{2880}$ versus temperature for pure DPPC liposomes. The transition temperature is measured on the profiles at the middle point of the transition region. DPPC presents a sharp transition at 41.3 ± 0.4 °C, a value which is very close to the T_m obtained by DSC (Fig. 2). Accuracy takes into account the resolution of the platinum probe used to measure temperature (0.1 Ω, corresponding to 0.3 °C) and the precision on the T_m determination from the experimental points (sigmoid fit).

3.2. UQn/DPPC liposomes

3.2.1. DSC study

Fig. 3 shows the heating thermograms of multilamellar vesicles of pure DPPC, and of mixtures containing the following UQ*n*/DPPC molar ratios: 0.01, 0.05 and 0.1. Globally, the presence of UQ*n* induces the broadening of the DPPC main transition, which may reflect a reduced cooperativity between the acyl chains of DPPC. However, the main transition of DPPC is much more affected by the presence of short-chain UQ*n* (UQ2 and UQ4) than by the long-chain ones (UQ6 and UQ10). Indeed, the higher the proportion of UQ2, the more the main transition peak (i) shifts towards lower temperatures, (ii) continuously broadens and (iii) decreases in intensity. The main phase transition peak for an UQ2/DPPC molar ratio of 0.10 shows two shoulders at temperatures about 37 and 38 °C. UQ4 has a less marked effect than UQ2. Moreover, the DPPC main transition is much less affected by UQ6 and, in the case of UQ10, no effect on the transition is observed.

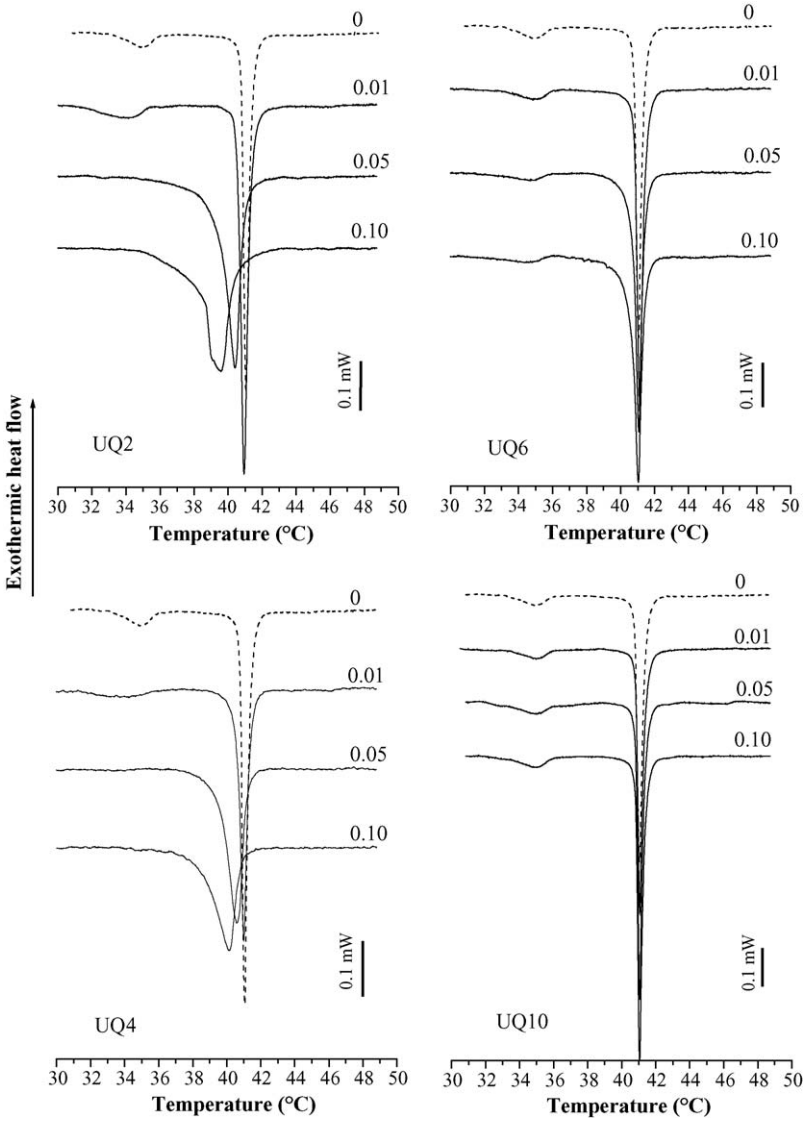

Fig. 3. DSC heating thermograms of multilamellar vesicles as a function of the UQ*n*/DPPC molar ratio indicated.

DSC profiles (Fig. 3) indicate that the pretransition of DPPC MLV is also sensitive to the presence of ubiquinones. Indeed, with UQ2 and UQ4, the pretransition shifts towards lower temperatures when molar ratio is 0.01. For higher molar ratios, this transition completely vanishes. In the case of UQ6, the pretransition peak shifts towards the lower temperatures and its intensity decreases as the mole ratio increases. No effect on the pretransition is observed in the presence of UQ10.

The thermodynamic parameters of the main transition, T_m, $\Delta T_{1/2}$ and ΔH were deduced from thermograms, and plotted versus UQ*n* molar ratio, for all the four ubiquinones studied (Figs. 4 and 5 and Table 1).

T_m, linearly decreases with the UQ*n* molar ratio (Fig. 4). This effect is pronounced for short-chain ubiquinones (UQ2 and UQ4), while T_m is slightly or not affected at all by long-chain ones (UQ6 and UQ10). Indeed, ΔT_m (i.e., the difference between T_m with and without ubiquinone), is equal to 1.5 °C in the presence of 0.10 UQ2/DPPC molar ratio, while for the same proportion of UQ10, ΔT_m is null. The peak width at half-height, $\Delta T_{1/2}$, is approximately linearly dependent on the UQ*n* concentration (Fig. 5). The peak half-width is comparatively more affected by short-chain ubiquinones ($0.4 < \Delta T_{1/2} < 1.3$) than with long-chain ones ($\Delta T_{1/2} < 0.5$). Lastly, a significant increase of ΔH with the ubiquinone molar ratio is noted only in the presence of UQ2. A maximum value of 48 kJ mol^{-1} is reached at 0.05 UQ2 molar ratio. For the other UQ*n*, ΔH values are almost similar, especially in the presence of 0.05 and 0.10 UQ*n*/DPPC molar ratios. Surprisingly, with 0.01 molar ratio, we found close ΔH values with UQ4 and UQ10, but a signif-

Table 1
Enthalpy values of the main phase transition of UQ*n*/DPPC vesicles

UQ*n*/DPPC molar ratio (%)	UQ2	UQ4	UQ6	UQ10
ΔH (kJ mol^{-1})				
1	39 ± 1	26 ± 1	34 ± 1	28 ± 1
5	48 ± 1	33 ± 1	34 ± 1	30 ± 1
10	48 ± 1	31 ± 1	34 ± 1	32 ± 1

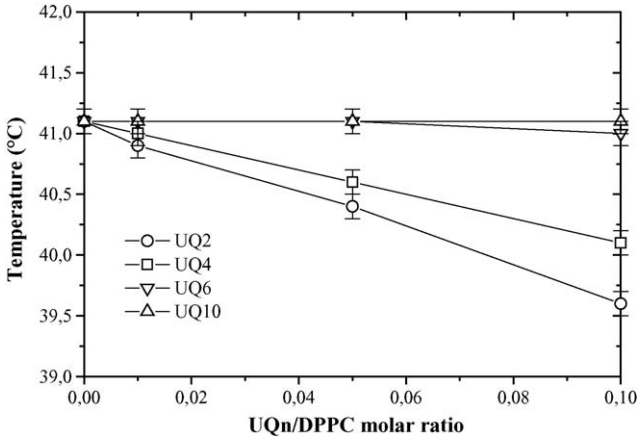

Fig. 4. Main transition temperature of mixed multilamellar vesicles obtained from DSC measurements as a function of the UQ*n*/DPPC molar ratio.

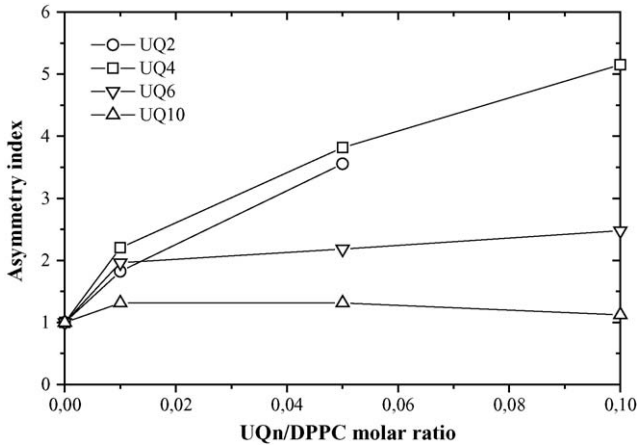

Fig. 6. Asymmetry index values of mixed multilamellar vesicles as a function of the UQ*n*/DPPC molar ratio.

icantly higher value with UQ6. However, it should be kept in mind that determined ΔH represents only an estimate of the transition enthalpy. Indeed, baseline subtraction, contribution of the wings of the transition and also accuracy on the sample mass determination, could render some apparent ΔH variations of several kJ mol^{-1} insignificant. Previously given accuracy (± 1 kJ mol^{-1}) determined by the sharp main transition of DPPC liposomes should be larger in case of mixed vesicles that should display a broader DPPC main transition. Consequently, only the large ΔH variations observed with UQ2/DPPC mixtures are considered to be significant.

To study the asymmetry changes of the main transition peak, we also plotted the asymmetry index, A_s, versus the UQ*n* molar ratio. A_s is defined by the following equation [44]:

$$A_s = \frac{[(T_{onset} - T_i)/(T_{endset} - T_i)]_{sample}}{[(T_{onset} - T_i)/(T_{endset} - T_i)]_{DPPC}}$$

T_{onset} and T_{endset} are the temperatures of the intercept between the base line and the tangent on the peak, respectively, in its increasing part (T_{onset}), in its decreasing part (T_{endset}). T_i is the interception point of these two tangents and its value is generally identical to T_m. If A_s is greater than 1, the peak is more asymmetric than for pure DPPC, while a value of A_s lower than 1 indicates than the peak is less asymmetric than the pure DPPC one. This A_s parameter is significant only in the presence of a single transition peak.

A_s was plotted versus the UQ*n* molar ratio for the four ubiquinones studied (Fig. 6). First, A_s is slightly affected by UQ10 and UQ6, since values are included between 1 and 1.3 for UQ10, 2 and 2.5 for UQ6. Second, A_s increased significantly with UQ2 and UQ4 amounts: its value reached 5 in the presence of 0.10 UQ4/DPPC molar ratio. Note that A_s could not be calculated for vesicles containing 0.10 UQ2/DPPC molar ratio, since the deconvolution process of the main transition peak (see Fig. 5) introduced accuracy and yielded meaningless A_s values.

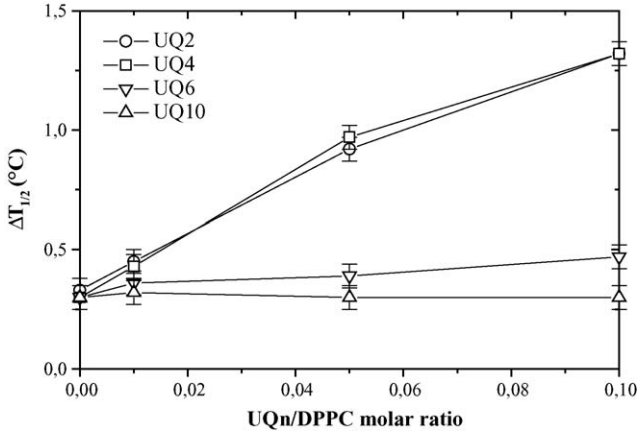

Fig. 5. Temperature width at half-height of mixed multilamellar vesicles as a function of the UQ*n*/DPPC molar ratio.

3.2.2. Raman analysis

Fig. 7 shows the Raman intensity ratio r (I_{2935}/I_{2880}) versus temperature for mixed liposomes containing the following UQ*n*/DPPC molar ratios: 0.01, 0.05 and 0.10.

In the presence of UQ*n*, the temperature profiles are shifted towards lower temperatures. This shift is more marked as the chain length of UQ*n* decreases. Indeed, plotting the main transition temperature versus UQ*n* molar ratio (Fig. 8), shows that the T_m is much more affected by the presence of UQ2 and UQ4 than with UQ6 and UQ10, as observed by DSC. In fact, for a 0.05 ubiquinone molar ratio, T_m values are 38.5 °C with UQ6 or UQ10, and only 35.7 °C in the presence of UQ2 or UQ4.

However, these T_m values are significantly different from those provided by DSC measurements, whereas both methods give similar data for pure DPPC liposomes. The Raman data show a much more noticeable effect of ubiquinones on modifying the main transition temperature than DSC. Hence, from calorimetric data, no influence of UQ10 on the main transition temperature ($T_m = 41.1$ °C) is observed, whereas Raman spectroscopy gives a T_m value lower than 38 °C for 0.10 UQ10/DPPC molar ratio. Similarly, with 0.05 UQ2/DPPC molar ratio, DSC and Raman spectroscopy give main transition temperature values equal to 40.4 and 35.7 °C, respectively. Indeed, at 0.05 UQ*n*/DPPC molar ratio, the difference $T_m^{DSC} - T_m^{Raman}$ is 4.8 °C for UQ2 and UQ4, and 2.8 and 2.5 °C for UQ6 and UQ10,

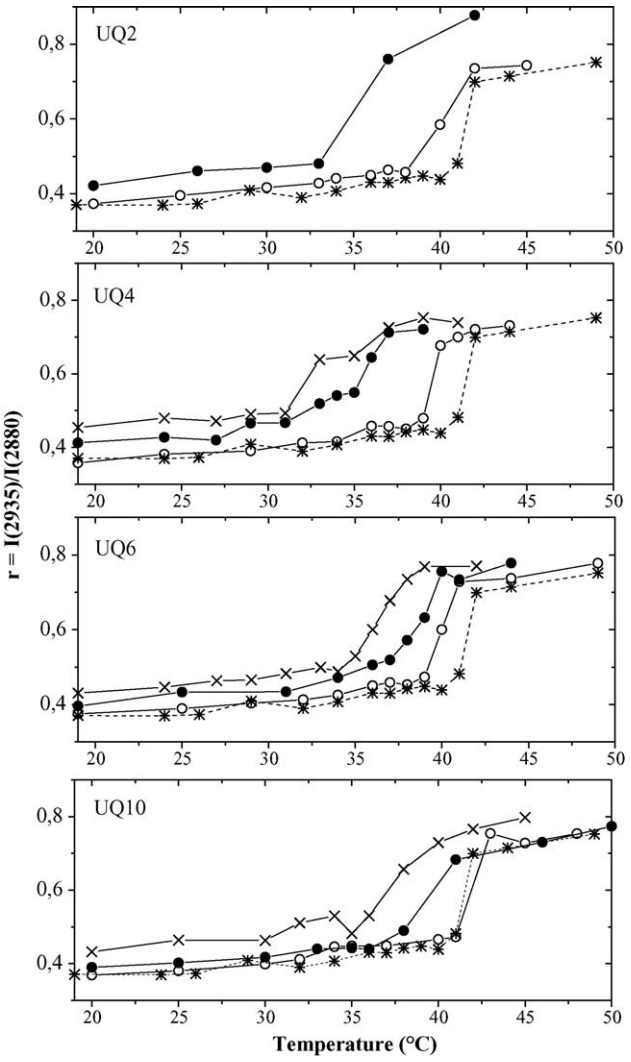

Fig. 7. Raman intensity ratio $r = I_{2935}/I_{2885}$ vs. temperature for mixed liposomes with different UQ*n*/DPPC molar ratios: (*) 0, pure DPPC; (◯) 0.01; (●) 0.05; (×) 0.1. The transition temperature was measured on the profiles at the middle point of the transition region.

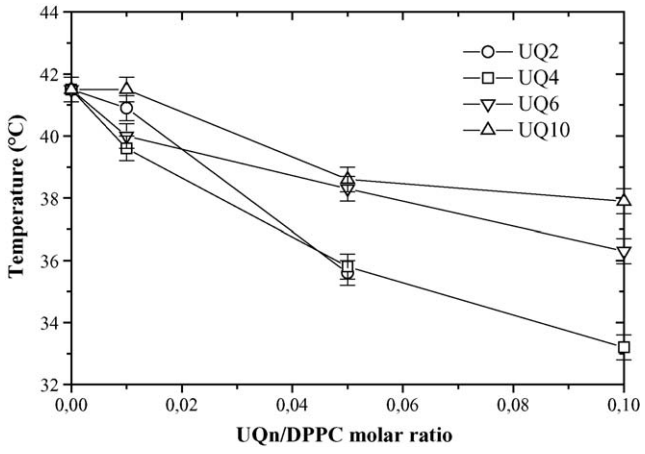

Fig. 8. Main transition temperature values of mixed multilamellar vesicles obtained from Raman spectra as a function of the UQ*n*/DPPC molar ratio.

respectively. This observed difference may be due to the contribution of isoprenoid chains in the vibrational coupling between adjacent chains revealed by the Raman intensity ratio r, especially by modifying the intensity of the $\nu_{as}(CH_2)$ mode located at 2880 cm^{-1}. Hence, during the main transition, positive values of $T_m^{DSC} - T_m^{Raman}$ correspond to a positive contribution of isoprenoid chains to the *r* ratio at a given temperature. Thus, some vibrational uncoupling between isoprenoid chains and alkyl chains of phospholipids leads to an artificial increase of the interchains disorder. It is noteworthy that vibrational coupling between hydrocarbon chains of ubiquinones and phospholipids might lead to an increase of the order and to negative contributions to the Raman intensity ratio and then to negative values of $T_m^{DSC} - T_m^{Raman}$.

4. Discussion

Several studies have shown that the insertion of host molecules into lipid bilayers resulted in an increase of the average volume accessible to a single phospholipid molecule (i.e., the introduction of "free volumes") [32,45]. The system tends to maximize its entropy by filling free volume by *trans-gauche* isomerization, resulting in a decrease of the main transition temperature. Moreover, insertion of molecules in the bilayer can induce a decrease in the cooperativity of the transition, highlighted by the broadening of the peak (i.e., the increase in $\Delta T_{1/2}$.). The peak symmetry indicates that the compounds are rather soluble in one of the two phases. Jain and Wu [35] have shown that, during a transition phase, the location of foreign molecules in phospholipid bilayers can be deduced from the nature of the effect on this transition. By studying around 100 biologically interesting compounds (fatty acids, alcohols, electrolytes and ionophores), they have underlined that four types of effects could be generally observed, each one related to a precise localization of the additive in the bilayer.

4.1. UQ2 and UQ4

4.1.1. Transversal location within the liposomal bilayer

The presence of short-chain ubiquinones (UQ2 and UQ4) in phospholipid bilayers generates a decrease in T_m and an increase in $\Delta T_{1/2}$. According to the classification by Jain and Wu, these two ubiquinones could belong to type A [33,35] and be located in C_1–C_8 methylene region, parallel to the aliphatic chains of phospholipids. Their polar benzoquinone rings are probably oriented towards the interfacial zone between the hydrophobic and polar parts of the bilayer. Other authors have drawn the same conclusion by studying the localization of short-chain UQ*n* in phospholipid vesicles by fluorescence anisotropy [46] or by fluorescence spectroscopy and linear dichroism [24,30].

Moreover, the pretransition is highly sensitive to the presence of small quantities of UQ2 and UQ4 since such behavior is no longer detected for UQ*n* molar ratios higher than 1%. Other studies have shown [44] that the penetration of even a small amount of host substances into the hydrophobic core of bilayer could force phospholipids into a single conformational phase, probably the $P_{\beta'}$ rippled gel phase. This confirms that UQ2 and

UQ4 are inserted between the phospholipid aliphatic chains. Their benzoquinone rings could interact with phospholipid polar headgroups through dipole–dipole interactions.

Finally, two assumptions can explain why UQ2 has a more pronounced effect on the lipid thermotropic phase behavior than UQ4. On the one hand, its strong polar character could provide UQ2 molecule with a higher degree of penetration than UQ4 (i.e., its benzoquinone ring being closer to DPPC polar heads). On the other hand, the disturbing effect induced by the insertion of UQ4 molecules could be partly compensated by van der Waals interactions between isoprenoid chains and phospholipid hydrocarbon chains. In such case, both ubiquinones would have the same degree of penetration and only the relative importance of the van der Waals interactions would explain the noted differences. Interestingly, ΔH remains constant in the presence of UQ4, which could indicate that UQ4 is intercalated between DPPC acyl chains, with prominent hydrophobic interactions. On the contrary, significant increases of ΔH versus molar ratio are observed with UQ2 containing vesicles. These observations suggest that electrostatic interactions between UQ2 and PC polar heads are probably due to a higher degree of penetration of UQ2 than UQ4. Lastly, as previously noted, positive values of $T_m^{DSC} - T_m^{Raman}$ reflect a vibrational uncoupling between chains of both compounds, which is incompatible with DPPC-UQ*n* attractive van der Waals interactions.

4.1.2. Lateral organization

The effect of short-chain ubiquinones on the broadening of the lipid main transition peak is concentration dependent and reflects reduction in the cooperativity of the transition (i.e., a decrease of the average number of molecules per cooperative unit) [32]. During the main transition, the cooperative units of the minor phase of pure DPPC can be described as large, nearly circular and highly compact domains in which all molecules melt cooperatively [47]. Then, changes in size distribution might appear in the presence of ubiquinones, as observed by Bonora et al. with DPPC liposomes containing phtalate esters [45]. According to this model, ubiquinones are likely to stabilize the gel at liquid crystalline phase domain boundaries. Consequently, domains of the minor phase become more ramified and limited, while an increase in number and the non-homogeneity of the composition broaden of the main transition peak [32,44]. This interpretation is consistent with the results of a Monte-Carlo simulation used to study the effects of an anaesthetic on the phospholipid phase transition [48]. This study concluded that anaesthetic molecules preferentially lie in the boundary region between lipid clusters of different phases, giving rise to the formation of an increasing number of smaller size clusters. In addition, a skewing towards lower temperatures of the transition peak in the presence of UQ2 and UQ4 (increasing A_s), suggests that these ubiquinones are soluble in the liquid crystalline phase, with a gradient of concentrations from the surface down to the inner part of the domains [45]. Consequently, it can be argued that short-chain ubiquinones could induce such localized and enriched zones in biological membranes, even with a low overall concentration, which is of great importance since the functions of respiratory chains proteins are highly sensitive to their lipid environment, especially to ubiquinones [30].

4.2. UQ6 and UQ10

Surprisingly, UQ6 exerts a significantly less marked influence on thermodynamic parameters (T_m, $\Delta T_{1/2}$, ΔH, A_s) than UQ4 with its two isoprene units deficiency. Especially, the markedly weak T_m variation could indicate that the degree of penetration of UQ6 molecules is insignificant. Moreover, UQ10 molecules have no effect on the thermodynamic behavior of DPPC liposomes. Thus, UQ6 and UQ10 would be of type C according to the classification by Jain and Wu [33,35] and located at the core of the bilayer, interacting with the C_9–C_{16} methylene groups. The weak influence of UQ6 on the pretransition confirms that its insertion between the aliphatic chains is limited. The benzoquinone rings have to be confined between the C_9-C_{16} methylene groups, probably associated to each other in order to minimize their interactions with the hydrophobic environment. The isoprenoid chain of UQ6 molecule could remain anchored in the bilayer centre.

Regarding UQ10, unaffected thermotropic behavior indicates that molecules lie between the two leaflets, parallel to the bilayer plan with their interacting benzoquinone rings. Two nuclear magnetic resonance studies [21,22] had previously reached the same conclusion. On the other hand, some authors have suggested [46], on the basis of fluorescence anisotropy experiments, that the benzoquinone rings of UQ10 interact with the interfacial zone, while the isoprenoid chains remain anchored at the center of the bilayer. However, other studies based on fluorescence spectroscopy and linear dichroism measurements [24] have indicated that, even if their rings tend to oscillate, UQ10 stays longer between the two layers, parallel to the bilayer plane. Such elements are in keeping with our informative DSC and Raman data on the location and organization of ubiquinones within bilayers.

The endothermic peak at about 45 °C corresponding to the typical melting of UQ10 isoprenoid chains (data not shown) cannot be observed, thus indicating the absence of aggregation of UQ10 molecules, either within or outside the bilayer, in our experimental conditions and confirms the relevance of the proposed location model. Interestingly, some authors have studied the distribution of higher proportions (>0.10) of UQ10 within phospholipid bilayers and suggested that aggregate formation occurs for molar ratios higher than 0.20 [49]. Then, in our experiments (molar ratios below 0.10) we can argue for an homogeneous molecular dispersion of UQ10, and to a lesser extent of UQ6, between the two phospholipid leaflets. Such a specific organization and homogeneous molecular dispersion of long-chain ubiquinones within bilayers have some interesting implications with regards to their biological functions. Indeed, other long-chain natural polyisoprenoids, such as dolichol, tocopherol or squalene, were found to lie in or near the core of the lipidic bilayer, by means of DSC, X-ray diffraction and neutron diffraction experiments on lipid bilayers, respectively (see ref. [28] and references therein). Due to their specific transversal membrane organization, polyisoprenoids, like other branched lipids, were thought to play a crucial role in the inhibition of

proton leakage across biological membranes [50]. In fact, it seems obvious that long-chain ubiquinones are highly eligible candidates for this function in mitochondrial membranes since maintaining the electrochemical protons gradient is essential for ATP synthesis and other bioenergetic functions.

4.3. Conclusion

To conclude, we have shown that the influence of small quantities of ubiquinones on the thermotropic phase behavior of DPPC multilayer vesicles depends heavily on the isoprenoid chain length. Indeed, this effect is all the more marked as the ubiquinone lateral chain is short, and our data lead us to establish a clear distinction between short- (UQ2 and UQ4) and long-chain (UQ6 and UQ10) homologues. The former category exerts a strong influence on the thermodynamic parameters, whereas the latter has a very slight or even no influence at all. UQ*n* specific locations within the phospholipid bilayer obviously account for such effect. Short-chain ubiquinones are inserted parallel to phospholipid molecules, their benzoquinone ring close to the polar heads of the DPPC, while long-chain ones would be localized at the center of the bilayer. Additionally, we have underlined a difference in the lateral organization since long-chain ubiquinones remain homogeneously dispersed within the bilayer, whereas short-chain ones are self-organized in highly concentrated regions localized at the boundary of lipid domains. Finally, it is interesting that mid-chain analogues, UQ4 and UQ6, exhibit fully distinct behaviors, while their lateral chains have a two isoprene unit difference.

These results support the hypothesis that such a chain length organization dependence may occur in biomembranes too with related consequences for the biological activities of the different UQ*n* homologues. Our conclusions clearly suggest that natural long-chain ubiquinones are more efficient than short-chain homologues against proton leakage across membranes. On the other hand, the specific organization of short-chain ubiquinones, especially their capacity for lateral segregation, can enhance their interactions with respiratory chain proteins, and subsequently the overall processes. Interestingly, this property can be correlated with the prominent therapeutic efficiency of short-chain exogenous ubiquinones observed in some clinical studies. Consequently, the biological activity of ubiquinone analogues is largely modulated by their physico-chemical properties that are mainly dependent on the isoprenoid chain length. Thus, the nature of the lateral chain of ubiquinone homologues constitutes a crucial criterion for selecting of new therapeutic derivatives.

References

[1] F.L. Crane, Y. Hatefi, R.L. Lester, C. Widmer, Biochim. Biophys. Acta 25 (1957) 220–221.
[2] R.A. Morton, G.M. Wilson, J.S. Lowe, W.M.F. Leat, Biochem. J. 68 (1958) 16.
[3] L. Ernster, G. Dallner, Biochim. Biophys. Acta 1271 (1995) 195–204.
[4] T.E. King, in: C.H. Kim, T. Ozawa (Eds.), Bioenergetics: Molecular Biology, Biochemistry and Pathology, Plenum Press, 1990, pp. 25–38.
[5] G. Dallner, P.J. Sindelar, Free Radic. Biol. Med. 29 (2000) 285–294.
[6] I.E. Scheffler, Mitochondria, John Wiley & Sons Inc., 1999.
[7] B. Soballe, R.K. Poole, Microbiology 145 (Pt 8) (1999) 1817–1830.
[8] M.D. Collins, *In* Methods in Microbiology, Academic Press, London, 1985, pp. 329–363.
[9] G.P. Moss, Nomenclature of Quinones with Isoprenoid Side-Chains—Recommendations 1973, vol. 2002, IUPAC-IUB Commission on Biochemical Nomenclature, 1973.
[10] U. Brandt, B. Trumpower, Crit. Rev. Biochem. Mol. 29 (1994) 165–197.
[11] H. Nohl, L. Gille, K. Staniek, Ann. N. Y. Acad. Sci. 854 (1998) 394–409.
[12] B. Frei, M.C. Kim, B.N. Ames, PNAS 87 (1990) 4879–4883.
[13] E. Niki, Mol. Aspects Med. 18 (1997) s63–s70.
[14] V.E. Kagan, J.P. Fabisiak, P.J. Quinn, Protoplasma (2000) 11–18.
[15] F.L. Crane, P. Navas, Mol. Aspects Med. 18 (1997) S1–S6.
[16] F.L. Crane, Protoplasma (2000) 127–133.
[17] C. Gomez-Diaz, M.P. Barroso, P. Navas, Protoplasma (2000) 19–23.
[18] R. Alleva, M. Tomasetti, L. Andera, N. Gellert, B. Borghi, C. Weber, M.P. Murphy, J. Neuzil, FEBS Lett. 503 (2001) 46–50.
[19] T. Kagan, C. Davis, L. Lin, Z. Zakeri, Ann. N. Y. Acad. Sci. 887 (1999) 31–47.
[20] S. Bernard, Y. Roche, F. Etienne, P. Peretti, Mol. Cryst. Liq. Cryst. 338 (2000) 207–221.
[21] E.L. Ulrich, M.E. Girvin, W.A. Cramer, J.L. Markley, Biochemistry 24 (1985) 2501–2508.
[22] G. Metz, K.P. Howard, W.B.S. van Liemt, J.H. Prestegard, J. Lugtenburg, S.O. Smith, J. Am. Chem. Soc. 117 (1995) 564–565.
[23] G. Lenaz, B. Samori, R. Fato, M. Battino, G. Parenti Castelli, I. Domini, Biochem. Cell. Biol. 70 (1992) 504–514.
[24] B. Samori, G. Lenaz, M. Battino, G. Marconi, I. Domini, J. Membr. Biol. 128 (1992) 193–203.
[25] H. Katsikas, P.J. Quinn, BBA-Biomembranes 689 (1982) 363–369.
[26] M. Jemiola-Rzeminska, B. Mysliwa-Kurdziel, K. Strzalka, Chem. Phys. Lipids 114 (2002) 169–180.
[27] T. Hauss, S. Dante, T.H. Haines, N.A. Dencher, BBA-Bioenergetics 1710 (2005) 57–62.
[28] T. Hauss, S. Dante, N.A. Dencher, T.H. Haines, BBA-Bioenergetics 1556 (2002) 149–154.
[29] Y. Roche, P. Peretti, S. Bernard, BBA-Biomembranes 1756 (2006) 468–478.
[30] G. Lenaz, FEBS Lett. 509 (2001) 151–155.
[31] M. Turunen, J. Olsson, G. Dallner, BBA-Biomembranes 1660 (2004) 171–199.
[32] R.L. Biltonen, D. Lichtenberg, Chem. Phys. Lipids (1993) 129–142.
[33] R.N. McElhaney, Chem. Phys. Lipids (1982) 229–259.
[34] K.M.G. Taylor, R.M. Morris, Thermochim. Acta 248 (1995) 289–301.
[35] M.K. Jain, N.-Y. Wu, J. Membr. Biol. 34 (1977) 157–201.
[36] K. Brandenburg, P. Garidel, J. Howe, J. Andra, L. Hawkins, M.H.J. Koch, U. Seydel, Thermochim. Acta 445 (2) (2006) 133–143.
[37] I.W. Levin, E. Keihn, W.C. Harris, Biochim. Biophys. Acta 820 (1985) 40–47.
[38] T.J. O'Leary, I.W. Levin, J. Phys. Chem. 88 (1984) 1790–1796.
[39] T. Lefèvre, M. Picquart, Biospectroscopy 2 (1996) 391–403.
[40] R. Mendelsohn, D.J. Moore, Chem. Phys. Lipids 96 (1998) 141–157.
[41] D. Chapman, F.M. Goni, in: F.D. Gunstone, J.L. Harwood, F.B. Padley (Eds.), The Lipid Handbook, 1994.
[42] A. Tahir, C. Grabielle-Madelmont, C. Betrencourt, M. Ollivon, P. Peretti, Chem. Phys. Lipids 103 (1999) 57–65.
[43] I.W. Levin, in: W.F. Murphy (Ed.), Proceedings of the Seventh International Conference Raman Spectroscopy, North-Holland, Amsterdam, 1980.
[44] S. Bonora, L. Ercoli, A. Torreggiani, G. Fini, Thermochim. Acta 385 (2002) 51–61.
[45] S. Bonora, G. Fini, B. Piccirilli, J. Therm. Anal. Calorim. 61 (2000) 731–743.
[46] M. Jemiola-Rzeminska, J. Kruk, M. Skowronek, K. Strzalka, Chem. Phys. Lipids 79 (1996) 55–63.
[47] W.W. van Osdol, Q. Ye, M.L. Johnson, R.L. Biltonen, Biophys. J. 63 (1992) 1011–1017.
[48] K. Jorgensen, J.H. Ipsen, O.G. Mouritsen, D. Bennett, M.J. Zuckermann, Biochim. Biophys. Acta 1067 (1991) 241–253.
[49] H. Katsikas, P.J. Quinn, Eur. J. Biochem. 124 (1982) 165–169.
[50] T.H. Haines, Prog. Lipid Res. 40 (2001) 299–324.